University of Nebraska - Lincoln
DigitalCommons@University of Nebraska - Lincoln

US Department of Energy Publications | U.S. Department of Energy

2009

Kinetics of Uranium(VI) Desorption from Contaminated Sediments: Effect of Geochemical Conditions and Model Evaluation

Chongxuan Liu
Pacific Northwest National Laboratory, chongxuan.liu@pnl.gov

Zhenqing Shi
Pacific Northwest National Laboratory

John M. Zachara
Pacific Northwest National Laboratory, john.zachara@pnl.gov

Follow this and additional works at: http://digitalcommons.unl.edu/usdoepub

 Part of the Bioresource and Agricultural Engineering Commons

Liu, Chongxuan; Shi, Zhenqing; and Zachara, John M., "Kinetics of Uranium(VI) Desorption from Contaminated Sediments: Effect of Geochemical Conditions and Model Evaluation" (2009). *US Department of Energy Publications*. 237.
http://digitalcommons.unl.edu/usdoepub/237

This Article is brought to you for free and open access by the U.S. Department of Energy at DigitalCommons@University of Nebraska - Lincoln. It has been accepted for inclusion in US Department of Energy Publications by an authorized administrator of DigitalCommons@University of Nebraska - Lincoln.

Environ. Sci. Technol. **2009,** *43,* 6560–6566

Kinetics of Uranium(VI) Desorption from Contaminated Sediments: Effect of Geochemical Conditions and Model Evaluation

CHONGXUAN LIU,* ZHENQING SHI, AND JOHN M. ZACHARA

Pacific Northwest National Laboratory, Richland, Washington 99354, USA

Received March 5, 2009. Revised manuscript received June 12, 2009. Accepted July 15, 2009.

Stirred-flow cell experiments were performed to investigate the kinetics of uranyl [U(VI)] desorption from a contaminated sediment collected from the Hanford 300 Area at the U.S. Department of Energy Hanford Site, Washington. Three influent solutions of variable pH, Ca and carbonate concentrations that affected U(VI) aqueous and surface speciation were used under dynamic flow conditions to evaluate the effect of geochemical conditions on the rate of U(VI) desorption. The measured rate of U(VI) desorption varied with solution chemical composition that evolved as a result of thermodynamic and kinetic interactions between the solutions and sediment. The solution chemical composition that led to a larger disequilibrium between adsorbed U(VI) and equilibrium adsorption state yielded a faster desorption rate. The experimental results were used to evaluate a multirate, surface complexation model (SCM) that has been proposed to describe U(VI) desorption kinetics in the Hanford sediment that contained complex adsorbed U(VI) in mass transfer limited domains (Lui et al. *Water Resour. Res.* **2008**, *44*, W08413). The model was modified and supplemented by including multirate, ion exchange reactions to describe the geochemical interactions between the solutions and sediment. With the same set of model parameters, the modified model reasonably well described the evolution of major ions and the rates of U(VI) desorption under variable geochemical and flow conditions, implying that the multirate SCM is an effective way to describe U(VI) desorption kinetics in subsurface sediments.

Introduction

Kinetically controlled uranyl[U(VI)] desorption has been observed in various contaminated subsurface sediments (*1*−*6*). Recent spectroscopic and microscopic studies suggest that kinetic U(VI) desorption results from the mass transfer limitation of uranyl geochemical reactions including dissolution (*5, 7, 8*) and surface complexation (*1, 9*) in intragrain or intra-aggregate domains. Mass transfer limits the delivery of reactants and removal of products, leading to local disequilibrium of solution chemical composition and U(VI) speciation in the intragrain or intra-aggregate domains from those in bulk or flowing groundwater solutions. The disequilibrium, on the other hand, drives the mass transfer processes, leading to a complex coupling of mass transfer with geochemical reactions along the transport pathways.

* Corresponding author phone: (509) 371-6350; fax: (509) 376-6354; e-mail: Chongxuan.liu@pnl.gov.

Various models have been proposed to describe the kinetic behavior of U(VI) release from contaminated sediments including reactive diffusion (*5, 8*); a first-order rate with time-variable rate constants (*2*); multirate, linear sorption model (*4, 10*); and multirate, surface complexation model (SCM) (*1*). The diffusion-based models have the advantage of incorporating complex intragrain pore-network that restricts U(VI) and associated species mass transfer (*8*). The characterization of pore-network properties including pore size and connectivity, and local diffusion coefficients, however, is a significant challenge for the application of diffusion-based models.

The first-order rate model with time-variable rate constants (*2*) is an empirical approach that ignores U(VI) geochemistry affecting U(VI) sorption/desorption reactions and consequently has a limited applicability. The multirate, linear sorption model was developed to describe U(VI) desorption from contaminated sediments at the U.S. Department of Energy (DOE) Hanford Site, Washington, in solutions with a relatively constant chemical composition (*4*). The model utilizes multiple first-order rate expressions to simulate the diffusion process (*11*), and has frequently been used to describe mass transfer between sorbed and aqueous phases (e.g., refs *11*−*14*). The model, however, assumes that sorption and desorption reactions in the mass transfer domains can be described by a linear sorption isotherm. This limitation has recently been removed by replacing the linear sorption expression with a surface complexation model (*1*). The applicability of the multirate SCM, however, has not been rigorously tested under variable geochemical conditions that affect U(VI) aqueous and surface speciation reactions. Such variable geochemical conditions occur in certain field settings, such as at Hanford's 300 Area, where groundwater composition is variable as a result of Columbia river water intrusion at high river water stages (*15*).

In this study, a series of stirred-flow cell experiments were performed to investigate the kinetic behavior of U(VI) desorption from a contaminated sediment collected from the Hanford 300 Area at the U.S. Department of Energy (DOE) Hanford Site, Washington. Three influent solutions containing variable pH, Ca, and carbonate concentrations that affect U(VI) aqueous and surface complexation reactions were injected into the reactor under dynamic flow conditions to evaluate the evolution of geochemical compositions and its effect on U(VI) desorption. The experimental results were used to define a thermodynamic and kinetic model to simulate the changes of chemical compositions as a result of solution-sediment interactions, and to evaluate the applicability of the multirate SCM to describe U(VI) desorption kinetics under variable geochemical conditions.

Materials and Procedures

Sediment. The sediment used in this study was collected from the capillary fringe beneath Hanford's 300 Area North Process Pond at a depth of about 3 m below ground surface (*16*). The sediment was contaminated by U(VI)-containing nuclear fuel fabrication liquid wastes that infiltrated the vadose zone beneath the North Process Pond during the period 1941−1973. Spectroscopic analysis revealed that U in the sediment primarily existed as adsorbed uranyl carbonate (>$SOUO_2HCO_3$) and hydroxide (>SOUOH) species that were exclusively associated with the <2 mm size fraction (*1*). The dry-sieved, < 2 mm size fraction, which contains 47.8 nmol/g of U (*1*), was therefore used in this study to investigate U(VI) desorption kinetics.

10.1021/es900666m CCC: $40.75

© 2009 American Chemical Society

Published on Web 08/10/2009

This article is a U.S. government work, and is not subject to copyright in the United States.

Desorption Experiment. The desorption of U(VI) from the sediment was investigated in a stirred-flow cell reactor (8 mL) using three U(VI)-free, synthetic groundwater (SGW) solutions (Supporting Information (SI) Table S1). The pH, Ca and carbonate concentrations that have major effects on U(VI) speciation were varied in these solutions: SGW2 is low in pH and carbonate, and high in Ca; SGW3 is high in pH and carbonate, and low in Ca; and SGW1 composition is intermediate between those of SGW2 and SGW3. All the SGW solutions were prepared by continuously bubbling with air in suspensions of calcite for at least one week before use to ensure equilibrium with atmospheric CO_2(g) and calcite. The equilibrated solutions were filtered (3 nm pore size) and stored in plastic bottles for the desorption experiments.

The flow cell reactor has an influent port at bottom and effluent port on top of the reactor. A 0.2 μm pore size membrane was fixed on the effluent port to retain the sediment in the reactor. The flow cell experiments were performed with a solid/water ratio of 131 g/L with a flow rate of 19.8 mL/hour that was controlled by a high-pressure gradient piston pump (Cole-Parmer, IL). The sediment suspension in the reactor was maintained by a magnetic stir bar. An intermittent flow and stop-flow (SF) technique with variable SF durations was applied to evaluate whether the U(VI) release from the sediment was equilibrium or kinetically controlled. The effluents were collected using an automatic fraction collector (Cole-Parmer, IL) for chemical measurements.

The effluent pH was measured immediately after sample collection. U(VI) in the effluent was analyzed with a kinetic phosphorescence analyzer with a detection limit of 0.001 μmol/L (Chemchek Instruments, Richland, WA). Effluent Ca, K, Mg, and Na were analyzed with inductively coupled plasma-optical emission spectrometer (ICP-OES) (Perkin-Elmer, Optima 2100DV). Total dissolved inorganic carbon was measured with a Dohrman carbon analyzer, DC-80.

Multirate SCM. The multirate SCM can be mathematically described as follows (*1*):

$$\frac{\partial C_i}{\partial t} + \frac{(1-\theta)\rho_s}{\theta}\sum_{j=1}^{N_s}\left(a_{ij}\sum_{k=1}^{M_j}\frac{\partial q_j^k}{\partial t}\right) = L(C_i), i = 1, 2, ..., N \quad (1)$$

$$\frac{\partial q_j^k}{\partial t} = \alpha_j^k(Q_j^k - q_j^k), j = 1,2, ..., N_s; k = 1, 2, ..., M_j \quad (2)$$

where C_i is the total aqueous concentration of chemical component i (mol/L); q_j^k is the concentration of adsorbed specie j at adsorption site k (mol/kg); a_{ij} is the stoichiometric coefficient of chemical component i in adsorbed species j; θ is the porosity; ρ_s is the solid density (kg/L); N is the total number of chemical components in aqueous phase; N_s is the total number of adsorbed species; M_j is the total number of adsorption sites for adsorbed species j; α_j^k is the rate constant of adsorbed species j at site k (h^{-1}); Q_j^k is the adsorbed concentration of species j at site k (mol/kg) in equilibrium with aqueous solution; and $L(C_i)$ is the transport term:

$$L(C_i) = F(C_i^{in} - C_i)/V \quad (3)$$

where F is the flow rate (mL/hour), V is the aqueous volume of the flow cell reactor (mL), and C_i^{in} is the total concentration of chemical component i in the influent solution. The equilibrium adsorbed concentration (Q_j^k) in eq 2 has to be calculated from the mass action equations of adsorption reactions (Table 1). Note that eq 2 becomes a commonly used multirate, linear sorption model (e.g., refs *11, 12, 14*) when Q_j^k is replaced by $f_k K_d C_j$, where K_d is the linear partitioning coefficient between aqueous and solid phases and f_k is the site fraction at site k.

TABLE 1. Surface Complexation and Ion Exchange Reactions Used in Modeling

surface complexation	log K^a
$>SOH + UO_2^{2+} + H_2O = >SOUO_2OH + 2H^+$	–4.29
$>SOH + UO_2^{2+} + CO_3^{2-} = >SOUO_2HCO_3$	16.66
Ion Exchange Reactions	
$Ca^{2+} + 2NaX = CaX_2 + 2Na^+$	1.88
$Mg^{2+} + 2NaX = MgX_2 + 2Na^+$	1.87
$K^+ + NaX = KX + Na^+$	1.32
$H^+ + NaX = HX + Na^+$	0.0

[a] Equilibrium constants for U(VI) surface complexation reactions were estimated in Liu et al. (*1*), from the batch data reported in Bond et al. (*6*), Equilibrium constants for ion exchange reactions were from McKinley et al. (*23*), based on Thomas-Gaines convention.

Results and Discussion

Evolution of Chemical Compositions. The effluent chemical compositions changed significantly as a function of time and influent solution (Figures 1−3). The initial effluent pH was consistently lower than that in the influent regardless of influent solution composition, which had a pH from 7.28 to 9.09 (SI Table S1). The observed initial pH decrease, which ranged from 0.4 to 0.9 pH unit relative to the influent pH values, was significant because a relative low solid/solution ratio (131 g/L) was used in this study. Assuming that the initial pH decrease was from the dilution of protons originally present in the sediment pore water by the influent solutions, then a mass balance calculation using an assumed 0.3 porosity, 8.2 wt % of the field sediment as the <2 mm size fraction (*1*), and a solid density of 2.76 g/cm^3 (*1*) gave a pH 4 for the pore water in the field sediment. Some of the protons in the sediment might have come from the ion exchange sites and mineral dissolution/precipitation reactions as discussed later. Nevertheless, the large initial drop of pH indicated that the sediment contained significant acidity that has not been neutralized despite over 30 years since the termination of liquid waste sources. The sediment acidity was apparently from the infiltration of the acidic nuclear fuels fabrication waste from the overlying process pond (*17*). Although bases were added for waste neutralization over 30 years ago, significant acidity has been preserved in the capillary fringe sediment.

The pH values in the effluents increased gradually with time, requiring 12 fluid residence times to reach the influent levels. Stop-flow events consistently led to a decrease in effluent pH immediately after SF events. These results collectively indicated that proton release from the sediment was a kinetic process that either resulted from the pH-buffering mineral dissolution/precipitation reactions and/or proton ion exchange process in the mass transfer-limited intra-aggregate domains.

The temporal changes of major cations in the effluent solution varied with influent solution. For SGW1 (Figure 1), all major cations (Ca, Mg, K, and Na) initially decreased with time, indicating that the soluble fraction of the cations in the sediment was higher than in the influent solution. The decrease of Mg and K concentrations was especially fast, and after one hour of elution their concentrations were below those in the influent solution. After the initial fast decrease, Mg and K concentrations gradually rebounded toward their influent levels. The effluent Ca and Na concentrations were consistently above or equal to their influent concentrations throughout the experiment. For the high Ca concentration SGW2 (Figure 2); Mg, K, and Na displayed an initial concentration pulse, followed by a slow decrease to influent levels. For high Na concentration SGW3 (Figure 3); Ca, Mg, and K displayed marked concentration decrease with time.

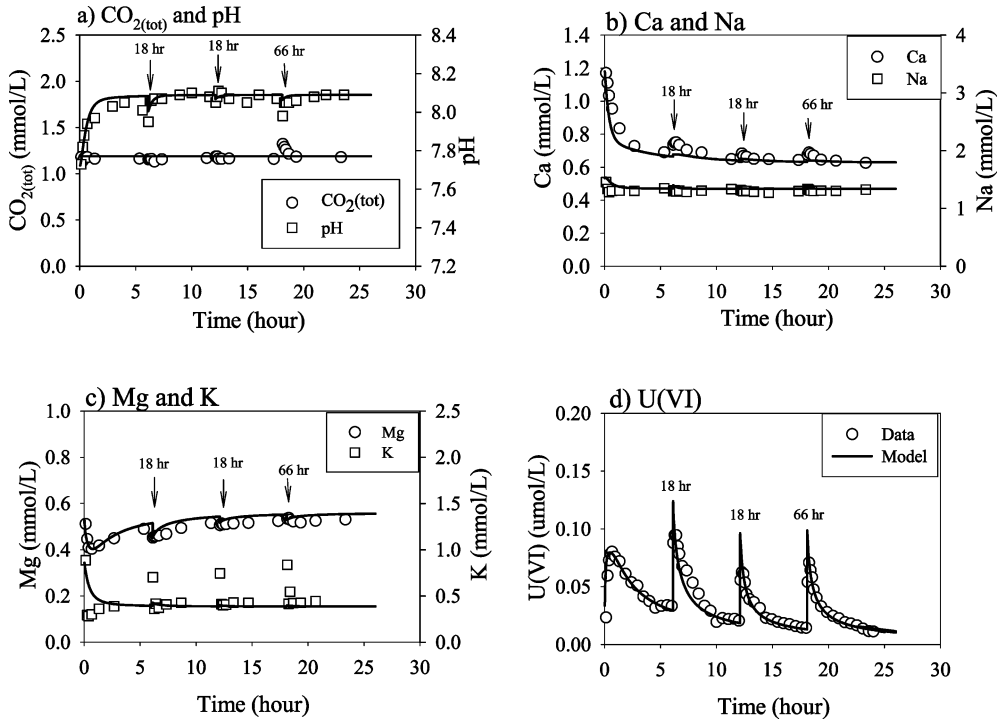

FIGURE 1. Temporal evolution of pH and aqueous inorganic carbon [CO_2(tot)] (a), Ca and Na (b), Mg and K (c), and U(VI) (d) in SGW1 effluent solutions during U(VI) desorption. Symbols are the experimental results and lines are the modeling results.

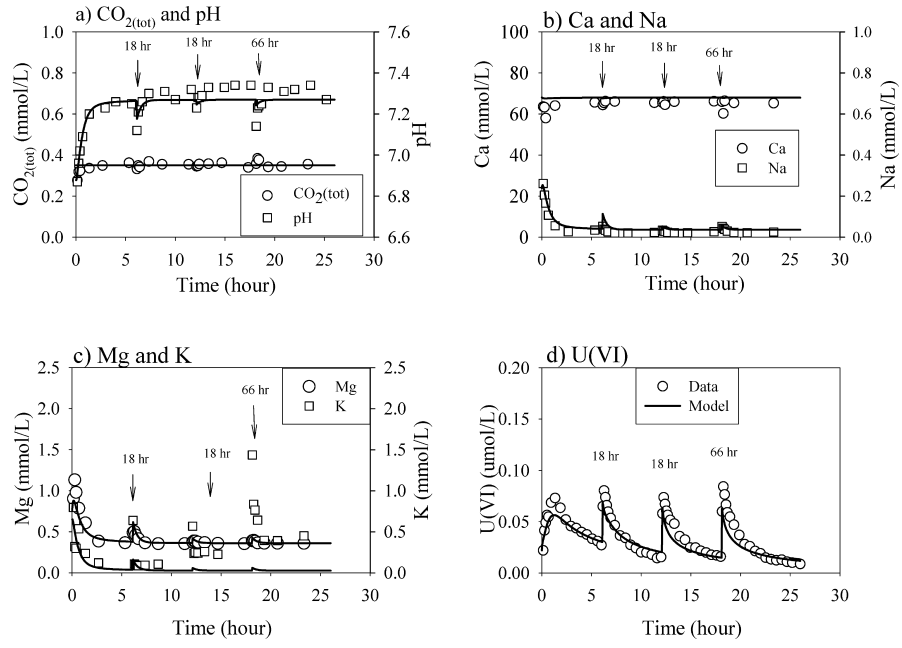

FIGURE 2. Temporal evolution of pH and aqueous inorganic carbon [CO_2(tot)] (a), Ca and Na (b), Mg and K (c), and U(VI) (d) in SGW2 effluent solutions during U(VI) desorption. Symbols are the experimental results and lines are the modeling results.

The temporal behavior of major cations was generally consistent with an ion exchange mechanism except during the first hour release, which was apparently affected by the dissolution of soluble salts. The correlated increase in Mg and K and decrease in Ca and Na concentrations after one hour elution in SGW1 (Figure 1) was explained by the exchange of solution Mg and K for the adsorbed Ca and Na in the sediment. As ion exchange approached equilibrium, all cation concentrations in the effluent approached those in the influent. The correlated increase in Ca, and decrease in Na, Mg, and K concentrations for SGW2 (Figure 2) indicated the exchange of aqueous Ca with adsorbed Na, Mg, and K in the sediment. Similarly, the correlated increase in Na and decrease in Ca, Mg, and K concentrations for SGW3 (Figure 3) indicated Na exchange replacing for sediment Ca, Mg, and K. In all these cases, significant time was required to reach ion exchange equilibrium with the influent solution, suggesting that these reactions were mass transfer-limited in intra-aggregate domains. The correlated increase or decrease in cation concentration immediately after SF events (e.g., Mg and Ca in Figure 1), and the presence of clay-textured aggregates and grain coatings in the sediment (*16*) supported such a kinetic mechanism.

The changes in carbonate concentration between influent and effluent solutions were relatively small. Calculations of aqueous speciation and saturation indexes indicated that all

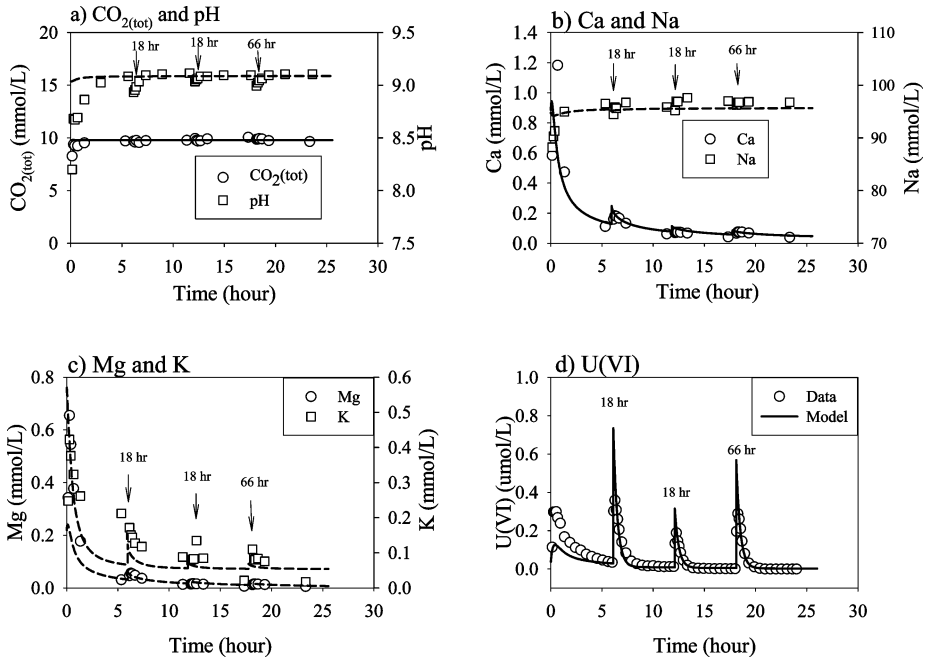

FIGURE 3. Temporal evolution of pH and aqueous inorganic carbon [CO_2(tot)] (a), Ca and Na (b), Mg and K (c), and U(VI) (d) in SGW3 effluent solutions during U(VI) desorption. Symbols are the experimental results and lines are the modeling results.

three influent SGW solutions were near calcite saturation with a saturation indices (log IAP/K_{sp}) ranging from −0.02 to 0.1. Slight changes in effluent carbonate concentration occurred within the first hour, and immediately after SF events. These changes probably resulted from the minor desorption of sorbed carbonate from mineral surfaces (e.g., refs *18, 19)* or the dissolution/precipitation of carbonate phases with different solubility from calcite. Generally however, such changes were small and in the following model, solid phase reactions for carbonate release were not considered except for the surface complexation of uranyl−carbonate species.

U(VI) Desorption. U(VI) desorption was fastest in SGW3 (Figures 1 to 3) because of its high pH and carbonate concentration that thermodynamically favored U(VI) in aqueous phase according to the U(VI) surface complexation reactions (Table 1). Effluent mass balance calculations (data not shown) also indicated that U(VI) desorption in SGW1 was 20% faster than that in SGW2. The result was also consistent with the thermodynamic potential effect on U(VI) desorption kinetics, because both pH and carbonate concentration were lower in SGW2 than SGW1. Although the high Ca concentration in SGW2 promoted the formation of poorly sorbing $Ca_2UO_2(CO_3)_3$(aq), its effect on U(VI) desorption was minimized by the low concentration of CO_3^{2-}, which was collectively affected by pH and total carbonate. Speciation calculations indicated that aqueous U(VI) species were dominated by $Ca_2UO_2(CO_3)_3$ and $CaUO_2(CO_3)_2^{2-}$ in SGW1; by $Ca_2UO_2(CO_3)_3$ (aq) in SGW2; and by $UO_2(CO_3)_3^{4-}$ and $CaUO_2(CO_3)_2^{2-}$ in SGW3 (SI Figures S1−3).

In all effluent solutions, U(VI) concentrations decreased with time and rebounded immediately and significantly after SF events, consistent with the kinetic behavior of U(VI) desorption observed previously in column systems (*1, 4*). The rebounded concentrations from the later SF events were, however, lower than from the earlier SF events with a comparable SF duration. Increasing SF durations at later times had only small effects on the magnitude of the rebounding effluent U(VI) concentration. Beyond the SF spikes, the effluent U(VI) concentrations gradually decreased with time, with the fastest decrease observed in SGW3 and slowest in SGW2. These results displayed the effect of depletion rate of the adsorbed U(VI) in the sediment. There was an apparent balance between the effect of increasing SF duration, which provided more time for the kinetic release of U(VI), and the depletion of U(VI) from the kinetic sites with time, which decreased the thermodynamic driving force for U(VI) desorption. The total desorbed U(VI) at the end of the experiment was 35, 30, and 54% of the total initial U(VI) in the reactor in SGW1, SGW2, and SGW3, respectively.

Modeling. The measured solutes and U(VI) concentrations in the effluents (Figures 1−3) were used to evaluate the suitability of the multirate SCM approach in describing U(VI) desorption kinetics (eqs 1−2). Ten chemical components were considered in modeling, including UO_2^{2+}, CO_3^{2-}, Na^+, Ca^{2+}, Mg^{2+}, K^+, NO_3^-, H^+, >SOH, and NaX, where >SOH represents the surface complexation site and NaX represents ion exchange site occupied by Na^+. The model consists of 46 relevant aqueous species (SI Table S2), and 4 ion exchange and 2 uranyl surface complex species (Table 1). All aqueous speciation reactions were treated as equilibrium ones that were used to determine aqueous species concentrations and activities. The Davies expression was used in calculating aqueous activity coefficients.

The U(VI) surface complexation reactions were based on >SOUOH and >SOUHCO$_3$ as surface species (Table 1). As previously described, these two species were directly determined in the contaminated sediment using laser induced fluorescence spectroscopy (*1*). The SCM was used to calculate the adsorbed concentration in equilibrium with bulk solution composition (i.e., Q_j^k in eq 2):

$$Q^k_{\mathrm{SOUO_2OH}} = \frac{S_k K_{\mathrm{SOUO_2OH}} a(\mathrm{UO_2^{2+}})/a^2(\mathrm{H^+})}{1 + K_{\mathrm{SOUO_2OH}} a(\mathrm{UO_2^{2+}})/a^2(\mathrm{H^+}) + K_{\mathrm{SOUO_2HCO_3}} a(\mathrm{UO_2^{2+}}) a(\mathrm{CO_3^{2-}})} \quad (4)$$

$$Q^k_{\mathrm{SOUO_2HCO_3}} = \frac{S_k K_{\mathrm{SOUO_2HCO_3}} a(\mathrm{UO_2^{2+}}) a(\mathrm{CO_3^{2-}})}{1 + K_{\mathrm{SOUO_2OH}} a(\mathrm{UO_2^{2+}})/a^2(\mathrm{H^+}) + K_{\mathrm{SOUO_2HCO_3}} a(\mathrm{UO_2^{2+}}) a(\mathrm{CO_3^{2-}})} \quad (5)$$

where S_k is the site concentration (mol/g) at site k, K is the equilibrium constant for adsorbed U(VI) species as described

TABLE 2. Initial Chemical Compositions and Rate Constants Used in Modeling

chemical	total labile[a]	ion exchange site[a]	surface complex site[b]
Na (mol/g)	5.73×10^{-6}	4.77×10^{-6}	
K (mog/g)	1.36×10^{-5}	9.83×10^{-6}	
Ca (mol/g)	6.47×10^{-5}	6.09×10^{-5}	
Mg (mol/g)	1.89×10^{-5}	1.81×10^{-5}	
H (mol/g)	5.92×10^{-7}	3.82×10^{-7}	
CEC[c] (cmolc/kg)		17.3	
$<SOUO_2OH$ (mol/g)			2.75×10^{-8}
$<SOUOHCO_3$ (mol/g)			2.03×10^{-8}
SC site[d] (mol/g)			7.83×10^{-5}
μ^e		−0.6	−5.8
σ^e		2.7	3.1

[a] Total labile and ion exchange cations were estimated from mass balance in the influent and effluents (see description in text). [b] Initial sorbed U(VI) species in the surface complexation site was estimated based on a method described in ref *1*. [c] Cation ion exchange capacity (CEC) was calculated from the summation of cations on ion exchange sites. [d] Surface complexation (SC) site concentration was estimated from a measured surface area of 20.4 g/m^2 and a site density of 3.84 umol/g. [e] Rate constants were estimated by fitting the effluent data in the SGW1experiment with an expected mean of 0.4 and 21 h^{-1} for U(VI) and ion exchange sites, respectively.

by the subscript, and a is the activity of aqueous species denoted in the bracket. With known aqueous activities in the bulk solution, the value $Q_j^k$for the two adsorbed U(VI) species can be calculated from eqs 4 and 5, which were derived by analytically solving the mass action equations of the surface complexation reactions (SI). The calculated Q_j^k was then used to calculate the rate of desorption from eq 2 based on the existing adsorbed concentrations (q_j^k) and the rate constant (α_j^k) at site k. The same rate constant was used for both U(VI) surface species. When the rate constant is infinitely large, q_j^k equals Q_j^k (eq 2) and desorption follows the Langmuir type expression (eqs 4 and 5).

Ion exchange reactions for cations Na^+, K^+, Mg^{2+}, Ca^{2+}, and H^+ (Table 1) were used to model the chemical composition evolution. The ion exchange kinetics were also assumed to follow eq 2. The ion exchange sites (X) were independent from the uranyl surface complexation sites (SOH) in accordance with the known mechanisms of these two different surface reaction types. The Q_j^k values for the ion exchange sites were analytically derived from the ion exchange mass action equations (SI). The same rate constant was used for all ionic species at the same exchange site.

The cation exchange capacity (CEC) and initial concentrations of exchangeable cations were estimated from cation concentration differences in the influent and effluent solutions. To minimize calculation errors, exchangeable Ca and Mg were estimated from the effluent data of the SGW3 experiment (Figure 3), as SGW3 contained negligible influent Ca and Mg. Exchangeable Na and K were estimated from the effluent data of the SGW2 experiment, as SGW2 contained minimal influent Na and K. The concentration differences between the effluents and influents were considered to represent the total sediment-associated labile cation pool, including soluble ones in the original pore water and exchange phase cations. Soluble cations were estimated from the first measured effluent cation concentrations in the SGW1 experiment (Figure 1). The exchangeable cations were estimated from the difference between the total sediment-associated and soluble cations (Table 2). The soluble and initially adsorbed proton concentrations in the sediment were estimated by fitting the effluent pH data for the SGW1 experiment. The CEC of the sediment was calculated by summing the concentrations of all initially exchangeable cations. After these initial conditions and parameters were estimated, they were fixed in simulating the effluent chemical compositions from all these experiments.

The surface complexation site concentration was calculated from a measured surface area of 20.4 m^2/g (*6*) and a generic surface site density of 3.84 umol/m^2 (*20*). The total measured contaminant U(VI) (T_{UO_2}) in the sediment (47.8 nmol/g) was treated as the initially adsorbed uranium concentration, which was assumed to be at thermodynamic equilibrium at all surface complexation sites. Based on this assumption, the initial concentrations of the two surface complex species (Table 2) were derived from the mass action equations of the surface complexation reactions as described elsewhere (*1*).

The rate constants (α_j^k) for the different sites in eq 2 were assumed to follow a log-normal probability distribution to minimize the number of parameters in the model:

$$p(\alpha) = \frac{1}{\sqrt{2\pi}\alpha\sigma}\exp\left(-\frac{1}{2\sigma^2}(\ln(\alpha) - \mu)^2\right) \quad (6)$$

where p is the probability of a site that has a corresponding rate constant of α; and μ and σ are the two parameters that define the probability function. Two probability functions were used: one for surface complexation sites, and another for ion exchange sites. For numerical convenience, the probability of each adsorption site was discretized to be a constant (e.g., $S_k = S_T/M_j$, where S_T is the total site concentration). The rate constant for each site was then calculated by inversely solving the probability function (eq 6). The discretization procedure of eq 6 was described in reference (*1*).

A sequential iterative scheme was used to numerically solve eqs 1 and 2 coupled with aqueous, surface complexation, and ion exchange reactions. Equation 1 was first implicitly solved for the total concentrations of all aqueous chemical components. The total concentrations were used to update the activities of aqueous species, which were then used to update the adsorption extent (Q_j^k). The new Q_j^k was used to update the adsorbed concentration (q_j^k) at each surface complexation and ion exchange site using eq 2. The updated q_j^k and Q_j^k were used to evaluate adsorption or desorption rates, which were then used to update eq 1 again. This process was iterated until convergence (relative error of 10^{-7}) for each time step.

The multirate SCM model, coupled with multirate ion exchange model, reasonably well described the effluent data with variable influent composition using a single set of parameters. The reaction constants for the aqueous, uranyl surface complexes, and cation exchange species were derived from literature and independent studies using the Hanford sediments (Table 1 and SI Table S2). The kinetic parameters (μ and σ in Table 2) for the rate distribution of ion exchange and surface complexation sites were estimated by visually fitting the model to the SGW1 effluent data (Figure 1). The fitted kinetic parameters were then used to predict the effluent compositions and U(VI) desorption profiles in the SGW2 and SGW3 experiments (Figures 2 and 3) as a validation. Correspondent calculated U(VI) aqueous speciation in the different reactors was provided in SI Figures S1−S3.

The model well described the evolution of Ca^{2+}, Mg^{2+}, and Na^+ in the effluents as a function of time and influent solution (Figures 1 to 3), indicating that the kinetic behavior of these cations can be well simulated by a multirate, ion exchange process. The model also well matched the effluent pH for SGW1 and SGW2, but underestimated the pH in SGW3, suggesting that the proton release from the sediment was also controlled by other reactions that were not considered

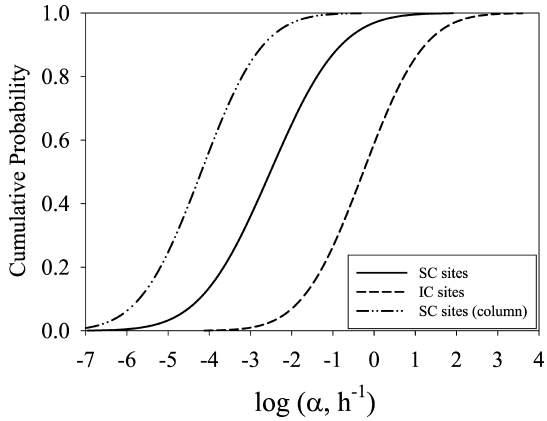

FIGURE 4. Accumulated probability of the first-order rate constants for ion exchange (IC) (short dashed line) and surface complexation (SC) sites (solid line) that were estimated by best fit of the effluent data in Figure 1. The dash-dot line represents a cumulated probability of the first-order rate constants for the SC sites estimated previously for this sediment in a column system (see text).

such as mineral dissolution/precipitation. The model was not effective in simulating the kinetic behavior of K release, but the ion exchange behavior of strongly adsorbing cations in the Hanford sediments is known to be complex because of the presence of basically weathered micas (*21*, *22*). The calculated K concentrations immediately after SF events were consistently less than the measured ones, regardless of SF duration and influent solution composition. The agreement between the K data and the model could not be improved by adjusting the equilibrium constant or the initial adsorbed K, without compromising the simulations of the other cations. The inability to accurately model K, however, had no direct effect on U speciation or its adsorption/desorption reactions as long as the modeled and measured Ca and Mg concentrations were in agreement. These latter two cations had strong influence on U(VI) aqueous speciation (SI Table S2).

The model generally provided a good description of U(VI) release as a function of time, chemical composition, and SF duration with the same set of initial conditions and model parameters. Some discrepancies did exist. For example, the model underestimated the SF effects for SGW2 (Figure 2), while it overestimated SF effects for SGW3 (Figure 3). The model match could be improved by adjusting the kinetic parameters to best fit the individual U(VI) effluent profiles (data not shown), indicating that the rate parameters (i.e., μ and σ) in the multirate SCM model were affected by fluid geochemical composition. This was expected because (1) the multirate SCM is a semiempirical model that describes U(VI) surface complexation reactions, diffusive mass transfer, and their coupling; and (2) only two parameters were used to describe the U(VI) mass transfer that occurred in complex and unresolved ways in intragrain and intra-aggregate regions in the sediment (*16*). Overall, however, the discrepancy between the calculated and measured U(VI) desorption profiles was not significant. Considering its simplicity in both numerical implementation and parametrization, the multirate SCM is recommended to be an effective approach to describe U(VI) desorption kinetics under variable geochemical conditions, with a caution that its rate parameters are not completely independent of geochemical conditions.

An evaluation of the probability function (eq 6) using the estimated rate parameters showed that the estimated rate constants ranged from 10^{-6} to 10^{1} h^{-1} for U(VI) surface complexation sites, and 10^{-3} to 10^{3} h^{-1} for ion exchange sites (Figure 4). Numerically, 50 sites were used for either U(VI) or ion exchange sites with a rate constant ranging from 2×10^{-6} to 4 h^{-1} for U(VI) sites, 1×10^{-3} to 3×10^{2} h^{-1} for ion exchange sites. The large ranges of rate constant distribution reflected the heterogeneous nature of the mass transfer properties for both U(VI) surface complexation and ion exchange reactions in the sediment. The overall rate for ion exchange sites was over 2 orders of magnitude faster than for uranyl surface complexation, suggesting that the ion exchange sites were more accessible and/or kinetically more responsive.

The rate constants determined for U(VI) surface complexation sites from the flow-cell experiments (Figure 4) were over 1 order of magnitude faster than those determined previously from a column containing the same sediment (*1*). The slower rates in the column system may have resulted from the additional intergrain mass transfer as a result of nonuniform distribution of flow velocity at the pore scale. Such intergrain mass transfer that occurred along with intragrain or intra-aggregate mass transfer, increased the overall mass transfer distance and slowed U(VI) release rates. In the stirred-flow system, the effect of intergrain mass transfer was intentionally eliminated by experimental design. The large increase in the rate constants in the stirred-flow system over that in the column was, however, unexpected and requires further investigation.

Implication. The kinetics of U(VI) adsorption/desorption is an important factor controlling uranium fate and transport at U-contaminated sites. A field investigation of reactive transport of U(VI) is currently underway at the Hanford Integrative Field Research Challenge (IFRC) Site at U.S. DOE Hanford 300 Area. At the site, significant variability in water composition is expected as a result of Columbia River water intrusion into groundwater at high water stage, and subsequent sediment-water interactions. Our results imply that such variability in groundwater chemical conditions will have significant effects on U(VI) adsorption/desorption kinetics and consequently, U(VI) concentration within the contaminant plume at the site. The desorption rate will be slowed in aquifer regions where groundwater is significantly diluted by relatively low carbonate and lower pH river water. The desorption rate will be fast toward inland regions where groundwater contains higher carbonate and pH. A dynamic kinetic scenario is expected when a plume of high U concentration moves from inland toward the river. In this scenario, both adsorption magnitude and desorption rate will be spatially variable in response to groundwater composition and mixing extent with river water. This scenario will be further complicated by the sediment-groundwater interactions that influence groundwater cation and bicarbonate concentrations, and by the seasonal changes in river stage that cause changes in head gradient and flow vectors.

A multirate SCM, that was supplemented with a multirate ion exchange model to describe the kinetic evolution of major cations and pH resulting from solution-sediment interactions, was evaluated for its ability to describe U(VI) desorption kinetics from a sediment that has experienced long-term U(VI) contamination. The model provided a good description of the experimental results that were generated under variable, but controlled geochemical conditions, implying that kinetic SCM was able to describe major ion effects on both the rate and extent of U(VI) adsorption/desorption reactions. However, discrepancies between the model and data were observed (Figures 2 and 3), as a result of the semiempirical nature of the model. The mass transfer rate parameters were also dependent, to a lesser degree, on the aqueous composition of the experimental systems. The applicability of such a model and model parameters will therefore require a full evaluation under field relevant conditions.

Acknowledgments

This research was supported by the U.S. Department of Energy (DOE) through the Environmental Remediation Science Division (ERSD) Science Focus Area (SFA) program and partially supported by the Integrative Field Research Challenge (IFRC) at Hanford 300 Area. PNNL is operated for the DOE by Battelle Memorial Institute under contract DE-AC06-76RLO 1830. We thank three anonymous reviewers for their constructive comments.

Supporting Information Available

Table S1 provides chemical compositions of three electrolytes used in the experiments. Table S2 lists aqueous speciation reactions used in the modeling of U(VI) desorption. Calculated U(VI) aqueous speciation in the stirred-flow reactor during flow and stop-flow periods, mathematical derivation of the equilibrium adsorbed concentration (Q_i^k k in eq 2) for the surface complexation site, and mathematical derivation of the equilibrium adsorbed concentration (Q_i^k k in eq 2) for the ion exchange site are also provided. This material is available free of charge via the Internet at http://pubs.acs.org.

Literature Cited

(1) Liu, C.; Zachara, J. M.; Qafoku, N. P.; Wang, Z. Scale-dependent desorption of uranium from contaminated subsurface sediments. *Water Resour. Res.* **2008**; *44*, W08413, DOI: 10.1029/2007WR006478.

(2) Braithwaite, A.; Livens, F. R.; Richardson, S.; Howe, M. T. Kinetically controlled release of uranium from soils. *Eur. J. Soil Sci.* **1997**, *48*, 661–673.

(3) Mason, C. F.; Turney, W. R.; Thomson, B. M.; Lu, N.; Longmire, P. A.; Chisholm-Brause, C. J. Carbonate leaching of uranium from contaminated soils. *Environ. Sci. Technol.* **1997**, *31* (10), 2707–2711.

(4) Qafoku, N. P.; Zachara, J. M.; Liu, C.; Gassman, P. L.; Qafoku, O.; Smith, S. C. Kinetic desorption and sorption of U(VI) during reactive transport in a contaminated Hanford sediment. *Environ. Sci. Technol.* **2005**, *39*, 3157–3165.

(5) Liu, C.; Zachara, J. M.; Qafoku, O.; McKinley, J. P.; Heald, S. M.; Wang, Z. Dissolution of uranyl microprecipitates from subsurface sediments at Hanford site, USA. *Geochim. Cosmochim. Acta* **2004**, *68* (22), 4519–4537.

(6) Bond, D. L.; Davis, J. A.; Zachara, J. M., Uranium (VI) release from contaminated vadose zone sediments: Estimation of potential contributions from dissolution and desorption. In *Adsorption of Metals by Geomedia II: Variable Mechanisms, and Model Applications*; Barnett, M. O., Kent, D. B., Eds.; Elsevier: Amsterdam, Netherlands, 2008; pp 375−416.

(7) McKinley, J. P.; Zachara, J. M.; Liu, C.; Heald, S. M. Microscale controls on the fate of contaminant uranium in the vadose zone, Hanford site, Washington. *Geochim. Cosmochim. Acta* **2006**, *70*, 1873–1887.

(8) Liu, C.; Zachara, J. M.; Yantansee, W.; Majors, P. D.; McKinley, J. P. Microscopic reactive diffusion of uranium in the contaminated sediments at Hanford, USA. *Water Resour. Res.* **2006**, *42*, W12420, DOI: 10.1029/2006WR005031.

(9) Stubbs, J. E.; Veblen, L. A.; Elbert, D.; Zachara, J. M.; Davis, J. A.; Veblen, D. R. Newly recognized hosts for uranium in the Hanford Site vadose zone. *Geochim. Cosmochim. Acta* **2009**, *73*, 1563–1576.

(10) Yabusaki, S. B.; Fang. Y.; Waichler, S. R. Building conceptual models of field-scale uranium reactive transport in a dynamic vadose zone-aquifer-river system. *Water Resour. Res.* **2008**, *44*, W12403, DOI: 10.1029/2007WR006617.

(11) Haggerty, R.; Gorelick, S. M. Multiple-rate mass transfer for modeling diffusion and surface reactions in media with pore-scale heterogeneity. *Water Resour. Res.* **1995**, *31*, 2383–2400.

(12) Culver, T. B.; Hallisey, S. P.; Sahoo, D.; Deitsch, J. J.; Smith, J. A. Modeling the desorption of organic contaminants from long-term contaminated soil using distributed mass transfer rates. *Environ. Sci. Technol.* **1997**, *31*, 1581–1588.

(13) Valocchi, A. J. Use of temporal moment analysis to study reactive solute transport in aggregated porous media. *Geoderma* **1990**, *46*, 233–247.

(14) Villermaux, J. Chemical engineering approach to dynamic modeling of linear chromatography. A simple method for representing complex phenomena from simple concepts. *J. Chromatogr.* **1987**, *406*, 11–26.

(15) Peterson, R. E.; Freeman, E. J.; Murray, C. J.; Thorne, P. D.; Truex, M. J.; Vermeul, V. R.; Williams, M. D.; Yabusaki, S. B.; Zachara, J. M.; Lindberg, J. L., et al. *Contaminants of Potential Concern in 300-FF-5 Operable Unit: Expanded Annual Groundwater Report of FY2004*; Pacific Northwest National Laboratory: Richland, WA, 2005.

(16) Zachara, J. M.; Davis, J. A.; Liu, C.; McKinley, J. P.; Qafoku, N. P.; Wellman, D. M.; Yabusaki, S. B. *Uranium Geochemistry in Vadoze Zone and Aquifer Sediments from the 300 Area Uranium Plume, PNNL-15121*; Pacific Northwest National Laboratory: Richland, WA, 2005.

(17) Corbin, R. A.; Simpson, B. C.; Anderson, D. E.; Danielson, W. F.; J. G., F.; Jones, T. E.; Kincaid, C. T. *Hanford Soil Inventory Rev.1.; RPP-26744*; CH2M Hill Hanford Group, Inc: Richland, WA: 2005.

(18) Zachara, J. M.; Girvin, D. C.; Schmidt, R. L.; Resch, C. T. Chromate adsorption on amorphous iron oxyhydroxide in the presence of major groundwater ions. *Environ. Sci. Technol.* **1987**, *21*, 589–594.

(19) Villalobos, M.; Leckie, J. O. Surface complexation modeling and FTIR study of carbonate adsorption to goethite. *J. Colloid Interface Sci.* **2001**, *235*, 15–32.

(20) Davis, J. A.; Kent, D. B., Surface complexation modeling in aqueous geochemistry. In *Mineral-Water Interface Geochemistry, Reviews in Mineralogy*; Hochella, M. F., White, A. F., Eds. Mineralogical Society of America: Washington, DC, 1990; pp 177−260.

(21) Zachara, J. M.; Smith, S. C.; Liu, C.; McKinley, J. P.; Serne, R. J.; Gassman, P. L. Sorption of Cs^+ to Micaceous Subsurface Sediments from the Hanford Site, USA. *Geochim. Cosmochim. Acta* **2002**, *66*, 193–211.

(22) Liu, C.; Zachara, J. M.; Smith, S. C.; McKinley, J. P.; Ainsworth, C. C.; Desorption kinetics of radiocesium from the subsurface sediments at Hanford site, U. S. A. *Geochim. Cosmochim. Acta* **2003**, *67*, 2893–2912.

(23) McKinley, J. P.; Zachara, J. M.; Smith, S. C.; Liu, C. Cation exchange reactions controlling desorption of $90Sr^{2+}$ from coarse-grained contaminated sediments at the Hanford site, Washington. *Geochem. Cosmochim. Acta* **2007**, *71*, 305–325.

ES900666M